Available online at www.sciencedirect.com
ScienceDirect
Journal of Power Sources 162 (2006) 1226–1231
JOURNAL OF POWER SOURCES
www.elsevier.com/locate/jpowsour

Short communication

Experimental characterization of in-plane permeability of gas diffusion layers

J.P. Feser, A.K. Prasad, S.G. Advani *

Fuel Cell Research Laboratory, Department of Mechanical Engineering, University of Delaware, Newark, DE 19716-3140, USA

Received 30 June 2006; received in revised form 28 July 2006; accepted 31 July 2006
Available online 15 September 2006

Abstract

Recent studies indicate that PEM fuel cell performance may be strongly influenced by in-plane permeability of the gas diffusion layer (GDL). The current study employs a radial flow technique for obtaining in-plane permeability of GDLs, using either gas or liquid as the impregnating fluid. A model has been developed and experimentally verified to account for compressibility effects when permeability measurements are conducted using a gas. Permeability experiments are performed on samples of woven, non-woven, and carbon fiber-based GDL at various levels of compression using air as the impregnating fluid. Woven and non-woven samples are measured to have significantly higher in-plane permeability compared to carbon fiber paper at similar solid volume fractions.

Keywords: Permeability; GDL; Fuel cells; Measurements; Porous media; Radial flow

1. Introduction

The gas diffusion layer provides five key functions for a PEM fuel cell: mechanical support for the proton exchange membrane, electronic conductivity, heat removal, reactant access to the catalyst layers, and product removal from it. The latter two functions are intimately linked to convective mass transport into and out of the gas diffusion layer and, for smaller fuel cells, heat removal as well. Therefore, it should be expected that the permeability of the gas diffusion layer is a key measure of the material performance. Experiments performed by Williams et al. [1] provide a correlation between through-plane permeability and limiting current density. However, in a recent review on gas diffusion layer characterization, Mathias et al. [2] points to in-plane permeability as the relevant parameter in fuel cell performance, citing diffusion as the dominant mechanism for through-plane transport. The view that in-plane permeability should be more relevant has been reinforced analytically by Feser et al. [3] as well as numerically by Pharaoh [4], particularly with respect to PEM fuel cells that employ serpentine flow fields. Other studies which have observed the effects of channel-to-channel convection have reported improved performance at high current density [5–8], again confirming the importance of enhanced convection. This is particularly well documented in interdigitated flow fields since forced convection is the primary motivation for them. However, computational models of interdigitated flow fields have shown that for a given stoichiometric ratio, changes to GDL permeability have negligible effect on cell performance [9]. This is logical since the total reactant penetration at a given stoichiometry into the GDL is the same regardless of GDL permeability; by design, it is 100%. However, even in this case higher GDL permeability clearly reduces the pumping power needed to maintain the given stoichiometry and thus is advantageous; the reduction in pumping power is, of course, unique to flow fields which utilize forced convection such as interdigitated flow fields and to a lesser extent serpentine flow fields. The pumping requirements of a parallel flow field would remain unaltered by a raised permeability. Also it is worth noting that computational models do not completely model liquid water formation, the removal of which may be expedited by increased GDL permeability.

While three of the five key roles of the gas diffusion layer are improved with increased convection, the need for low electrical contact resistivity apparently requires a design trade-off; electronic resistivity is reduced substantially by increasing compressive force whereas permeability (and therefore reactant and product mass transport) is reduced by it [10]. Polarization curves

* Corresponding author. Tel.: +1 302 831 8975; fax: +1 302 831 3619.
E-mail address: advani@udel.edu (S.G. Advani).

0378-7753/$ – see front matter © 2006 Elsevier B.V. All rights reserved.
doi:10.1016/j.jpowsour.2006.07.058

obtained at various levels of compression confirm that this is an important optimization process in fuel cell operation [11]. Thus, it is also desirable to know how permeability changes with compression.

The preceding discussion identifies a need in the fuel cell community for methods to measure gas diffusion layer permeability at various compressive loadings. Transverse or through the thickness permeability is most commonly measured, and several techniques for its measurement have been described [2,12,13]. Fewer techniques have been used to characterize the in-plane permeability of the gas diffusion layer. This will be the focus of the present work. Mathias et al. [2] describes a method in which two flow channels can be used to determine the in-plane permeability by measuring the relationship between pressure gradient and flowrate. While this technique is valid, achieving the necessary sealing can be difficult in practice because of the rectangular geometry. An alternative method is to measure the flowrate–pressure relationship in a radial-flow apparatus through an annulus of GDL material; sealing difficulties are alleviated by constraining the upper and lower surfaces of the annulus between two sufficiently flat and smooth plates. This measurement technique has been utilized in characterizing textile preforms in composites manufacturing [14–16]. However, the impregnating fluid is usually a viscous incompressible liquid. This method was recently adopted by Bluemle et al. [13] who compressed gas diffusion layers to measured force loadings in an Instron machine and determined their in-plane permeability by passing compressed air through an annulus while measuring flowrate and pressure drop across the layers. Assuming incompressibility of the gas and using Darcy's law, permeability was obtained from a least-squares fit of the data. An interesting aspect of this work is that the Darcy–Forchheimer convection model was used so that the experiment yielded both the viscous (Darcy) permeability and the inertial permeability. However, this was done only for through-plane permeability measurements as the inertial permeability was undetectable within the error bounds of measurement for the in-plane portion of that study. The current work had a similar experience with in-plane measurements.

The current work presents improvements to the existing techniques which allow in-plane permeability to be measured more accurately and with increased flexibility. Several difficulties arise in measuring in-plane permeability. First, the thickness of the gas diffusion layer can be quite small (some are as thin as 100 μm). This is on the same order of magnitude of typical machining tolerances; thus, any testing apparatus made by conventional techniques will introduce an element of uncertainty into the measurements due to uneven compression on the GDL leading to potential 'short-circuiting' pathways for the penetrating fluid. In the current study, an attempt is made to circumvent this effect by stacking multiple layers of material during experiments. For example, stacking eight layers of a 100 μm material raises the total thickness to 800 μm, for which a realistic machining tolerance of 25 μm allows the GDL to follow the contours of the machined surface to within about 3% of the total GDL thickness. To ensure that the 'nesting' between adjacent layers of GDL does not alter the outcome of the experiment, layers of thin, tightly toleranced shim stock can be used to separate each layer of the GDL stack.

A second difficulty addressed here is that because gas is used as the penetrating fluid, a truly compressible model of radially permeating flow should be used to fit the measured data. This is essential if the pressure difference used to drive the penetrating fluid is on the same order of magnitude as the absolute pressure of the fluid. An appropriate model, which is easily reducible to the incompressible case, is developed here for this purpose.

A third consideration that arises when measuring the permeability is that in order to have a well defined Darcy permeability, there should be a sufficient number of pores contained within the flow. For a typical gas diffusion layer, the majority of the void fraction is formed by pores between 10 and 100 μm in diameter [2]; thus, the distance traveled by the flow within the sample of material being tested should be on the length scale of centimeters for a reliable reading. It is interesting to note that most PEM fuel cells violate this principle since channel lands are typically about 1 mm wide, meaning that Darcy permeability is not strictly applicable on such length scales. To ensure that there are sufficient pores for consistent in-plane permeability measurements, the current study will employ much larger sample sizes than used in the Bluemle study [13]. Finally, an assumption is made that the in-plane permeability of the porous materials is transversely isotropic. The fabrics may exhibit slight degree of anisotropy in-plane but for practical purposes this can be ignored [17].

Using these improvements and assumptions, an apparatus was constructed and used to measure the in-plane permeability of several commonly available gas diffusion layers.

2. Measurement technique

2.1. Radial flow apparatus

A radial flow apparatus (Fig. 1) was fabricated to test samples of GDL for in-plane permeability at various levels of compressive strain. The samples consisted of annuli of material 15 cm o.d. × 9 cm i.d. stacked to a height of approximately 1 mm with each layer of material separated by a thin layer of brass shim stock (51 ± 5 μm each); as stated earlier, this was done to avoid nesting effects between stacked layers. Thicker shim stock was also used to control the total thickness of the compressed stack. For gas permeability experiments, compressed air (0–550 kPa) was introduced at the outer edge of the annular sample stack, forced through the sample in the in-plane direction, passed from the outlet at the center of the stack to a rotameter for flowrate measurement, and subsequently released into the atmosphere. In liquid permeability experiments, a pressurized tank (0–200 kPa) forced water though the sample and was collected in a graduated cylinder at the outlet. In the case of gas permeability, pressure was measured using gauges at both the inlet and the outlet as rotameters were found to introduce a significant pressure drop. For the case of liquid permeability, pressure was measured by a gauge on the inlet only and assumed to be atmospheric pressure at the outlet. The permeability measurement was accomplished by recording the pressure at approximately 10 different values of flowrate.

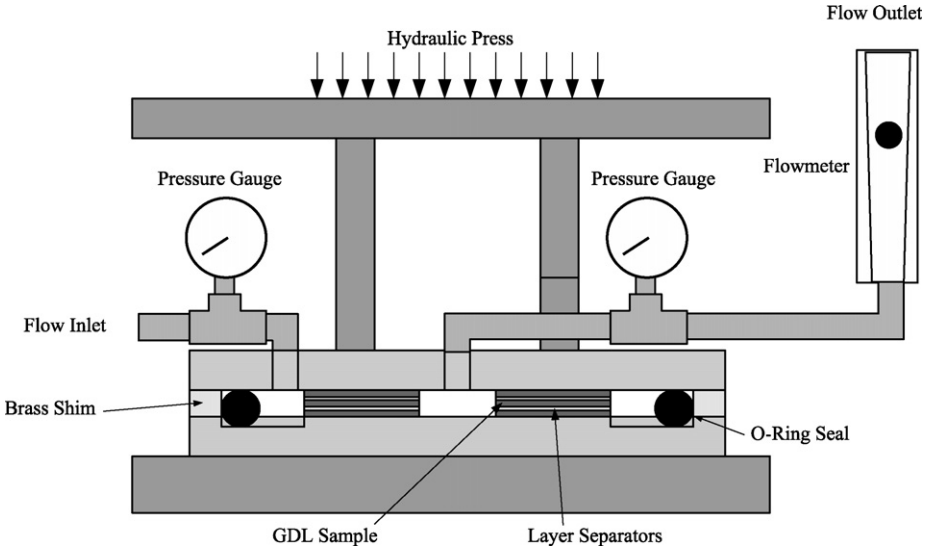

Fig. 1. Radial flow permeability testing apparatus.

2.2. Model

The collected data can be used to determine permeability once a model incorporating fluid compressibility is developed. For this purpose, we use Darcy's Law under the assumption that in-plane permeability is homogenous and transversely isotropic. In radial coordinates:

$$\bar{v} = -\frac{k_\mathrm{i}}{\mu}\frac{\mathrm{d}P}{\mathrm{d}r} \tag{1}$$

where $\bar{v}$ is the in-plane average fluid velocity, k_i the in-plane permeability, μ the fluid viscosity and $\mathrm{d}P/\mathrm{d}r$ is the radial pressure gradient. Mass conservation requires that in the annulus:

$$\frac{\mathrm{d}}{\mathrm{d}r}(\rho\bar{v}A) = 0 \tag{2}$$

where ρ is the fluid density and A is the cross-sectional area of the GDL sample as seen by the impregnating fluid. The density term has been retained in Eq. (2) because we intend to allow for compressibility effects which become important for large pressure variations. If Eqs. (1) and (2) are used in conjunction with the ideal gas law, then:

$$\frac{\mathrm{d}}{\mathrm{d}r}\left(\frac{P}{RT}\frac{k_\mathrm{i}}{\mu}\frac{\mathrm{d}P}{\mathrm{d}r}(2\pi rh)\right) = 0 \tag{3}$$

where h is the total thickness of the GDL sample stack (minus the separator shim between adjacent samples). The boundary conditions are $P(r_\mathrm{i}) = P_\mathrm{i}$ and $P(r_\mathrm{o}) = P_\mathrm{o}$, where pressure is measured in the absolute sense. In the absence of heat transfer to the solid surface and for changes in velocity small compared with the speed of sound, conservation of energy requires constant enthalpy. Under those assumptions, the process is thus regarded as isothermal. Integrating once:

$$rP\frac{\mathrm{d}P}{\mathrm{d}r} = C \tag{4}$$

Upon a second integration:

$$C = \frac{P_\mathrm{o}^2 - P_\mathrm{i}^2}{2\ln(r_\mathrm{o}/r_\mathrm{i})} \tag{5}$$

Then:

$$\frac{\mathrm{d}P}{\mathrm{d}r} = \frac{1}{rP}\frac{P_\mathrm{o}^2 - P_\mathrm{i}^2}{2\ln(r_\mathrm{o}/r_\mathrm{i})} \tag{6}$$

Now, we wish to relate the outlet flowrate to the pressure. Then:

$$Q_\mathrm{out} = (vA)_{r_\mathrm{o}} = \frac{\pi k_\mathrm{i} h}{\mu\ln(r_\mathrm{o}/r_\mathrm{i})}\frac{(P_\mathrm{i}^2 - P_\mathrm{o}^2)}{P_\mathrm{o}} \tag{7}$$

Eq. (7) is used to calculate permeability of the porous material based on measurements of P and Q. It should be noted that when the difference between the inlet and outlet pressures is small relative to the absolute pressures employed, Eq. (7) can be linearized in P and reduces to the more familiar equation:

$$Q_\mathrm{out} = \frac{2\pi k_\mathrm{i} h}{\mu\ln(r_\mathrm{o}/r_\mathrm{i})}(P_\mathrm{i} - P_\mathrm{o}) \tag{8}$$

which is used for incompressible fluids.

A key requirement of the aforementioned method is that the viscous resistance on the fluid due to the walls should be small compared to the viscous resistance due to the porous medium. To determine if wall effects are indeed negligible, it is useful to introduce the idea of 'permeability' between parallel discs (such as in the case of a hydrostatic bearing) for which the flowrate–pressure relation is well known and is given by

$$Q_\mathrm{out} = \frac{\pi h^3}{6\mu\ln(r_\mathrm{o}/r_\mathrm{i})}(P_\mathrm{i} - P_\mathrm{o}) \tag{9}$$

Comparing Eq. (9) with the form of Eq. (8), it is reasonable to define the permeability of parallel discs as

$$k_\mathrm{wall} = \frac{h^2}{12} \tag{10}$$

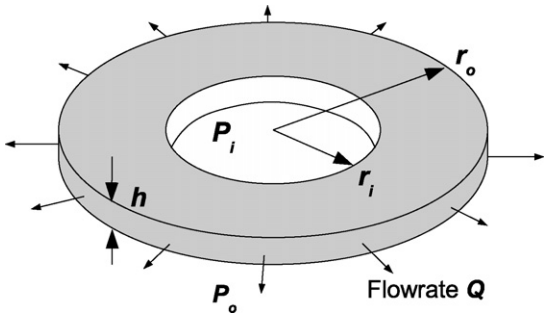

Fig. 2. Variables used for the model derivation.

Currently available gas diffusion layers have thicknesses in the range 100–500 μm. Thus, corresponding range of k_{wall} is 8×10^{-10} to 2×10^{-8} m^2. As will be seen, measured GDL permeability is substantially less than even the lower bound of wall permeability; thus, wall effects do not significantly influence the measurement (Fig. 2).

3. Validation

In order to determine the validity of Eq. (7), an experiment was conducted to verify that the permeability obtained using an incompressible fluid – for which the method is well known – matches the permeability obtained using a compressible fluid in conjunction with Eq. (7). A densely woven glass fabric annulus (15 cm o.d. × 9 cm i.d.) of initial thickness 600 μm was compressed to 380 μm and subjected to both a liquid and a gas permeability experiment. For the liquid permeability experiment, water was chosen as the fluid in order to achieve full wetting of the pores; a constant inlet gauge pressure of 180 kPa was used. The results are shown in Fig. 3 (air) and Fig. 4 (water).

The parabolic dependence of flowrate on pressure for compressible flow is clearly revealed by Fig. 3. Note that it is not possible to fit a straight line to the data that would fall within the error bounds of the data points. Instead, as suggested by Eq. (7), a parabola is found to fit the data very well. It should be noted that in the current study the flowrate data were collected over multiple orders of magnitude by multiple flowmeters resulting in error bounds that were not equal throughout the range of collection. Therefore, the residual scheme of the least squares method was modified to minimize the sum of the logarithm of the residuals rather than simply the residuals themselves. Using this scheme, the gas permeability of the glass fabric was determined to be $k_i = 5.89 \times 10^{-13}$ m^2. By comparison, liquid permeability data indicated the permeability of the same sample to be $k_i = 6.02 \times 10^{-13}$ m^2. Since the difference between the two measurements is quite small, it can be concluded that Eq. (7) is valid. It should also be noted that fitting gas permeability to the incompressible equation results in a gross over-estimation of permeability. This may have occurred in previous studies.

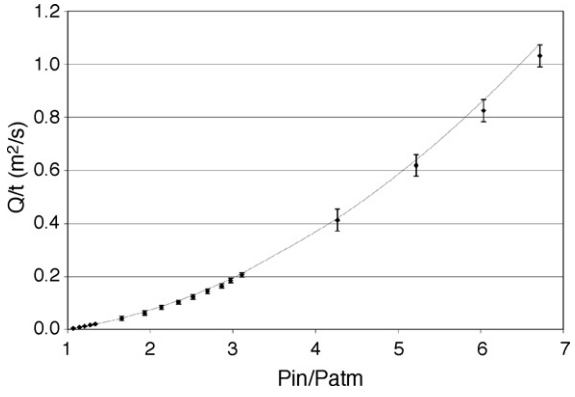

Fig. 3. Experimental data points for air as the impregnating fluid with tightly woven glass fabric as the porous medium. Solid line represents a non-linear least-squares fit of Eq. (7). Computed in-plane permeability value $k_i = 5.89 \times 10^{-13}$ m^2.

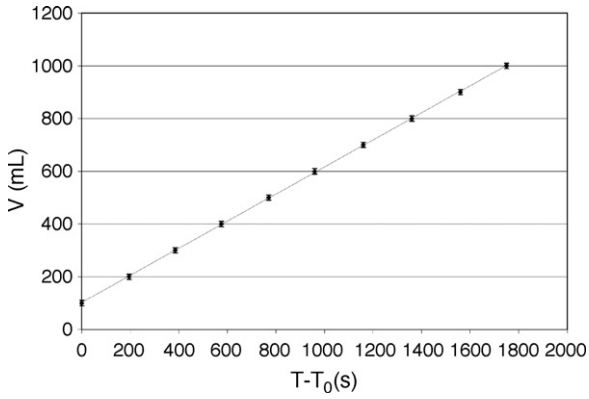

Fig. 4. Experimental data points with water as the impregnating fluid with tightly woven glass fabric as the porous medium. Solid line represents a least-squares fit of Eq. (8). Computed in-plane permeability value $k_i = 6.02 \times 10^{-13}$ m^2.

4. Measurements of GDL permeability

Permeability was measured for three types of gas diffusion layers, each representing one of the major manufacturing techniques: woven carbon fiber (cloth), non-woven carbon fibers, and carbon fiber paper shown in Fig. 5. Measurements were taken at multiple levels of compression typically used in fuel cells. The woven carbon fiber sample was Avcarb 1071-HCB (Ballard). The non-woven carbon fiber and paper-based samples were SGL31BA (SGL Carbon) and TGP-60-H (Toray), respectively. None of the samples contained a microporous layer. The initial thickness of each type of sample was determined with a micrometer gage. In order to prevent crushing of the sample by the gage, the thickness was measured by sandwiching the sample between two 2.5 cm × 2.5 cm square pieces of shim stock which helped to distribute the clamping force. The average of five measurements was taken as the initial thickness for each sample type. The measured initial thicknesses as well as the compression levels used during permeability experiments are shown in Table 1.

As described previously, multiple layers of GDL separated by thin spacers were used to increase flowrate and thickness to achieve the desired experimental accuracy. For all three material types, using four material layers was found to be sufficient and pressure–flowrate data were collected for each four-layer sample. Thickness fractions were incrementally decreased, reusing the sample until the lowest thickness fraction was reached. Then

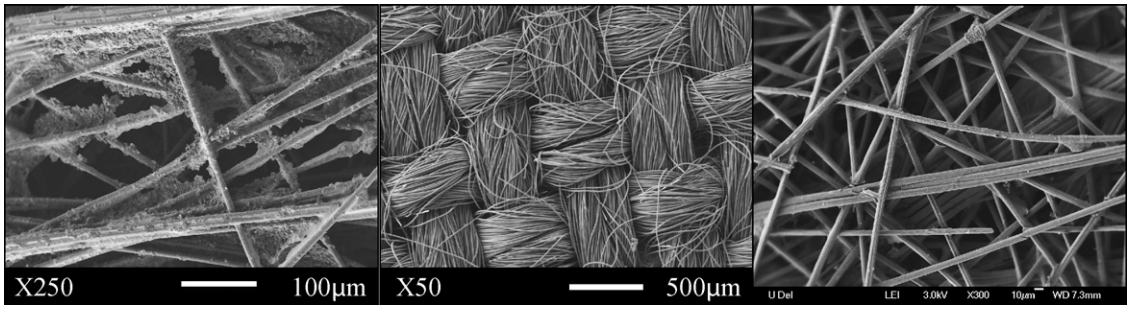

Fig. 5. SEM images of non-woven (left), woven (center), and carbon fiber paper (right) GDL materials.

the samples were replaced and the test was repeated. The test was repeated five times for each material type. Fig. 6 shows the average permeability for each material type at various levels of compression. The error bars indicate the 95% confidence interval based on the mean and standard deviation of the five experiments at each level. It was found that SGL31BA (non-woven) had a very similar range of permeability compared to Avcarb 1071-HCB (woven). This range of permeabilities is surprisingly high considering that Bluemle et al. [13] reports in-plane permeabilities about an order of magnitude lower for various ETEK woven cloth samples. Our data indicate that TGP-60-H (paper) has significantly lower permeability than the other materials; its measured range of permeabilities is in good agreement with the range reported by Mathias et al. [2]. Perhaps not surprising is that the woven material shows the most consistency in permeability from sample-to-sample; The non-woven and paper-based materials show permeabilities that have a variation in the range of 10–15% of the measured average compared to carbon cloth which shows a range of 5–10%.

Table 1
Sample types and conditions used during experiments

Sample	Initial thickness (μm)	Thickness fractions (%)
Avcarb 1071-HBC	335	94, 90, 86, 79, 73
SGL31BA	318	88, 82, 76
TGP-60-H	192	96, 90, 82, 76

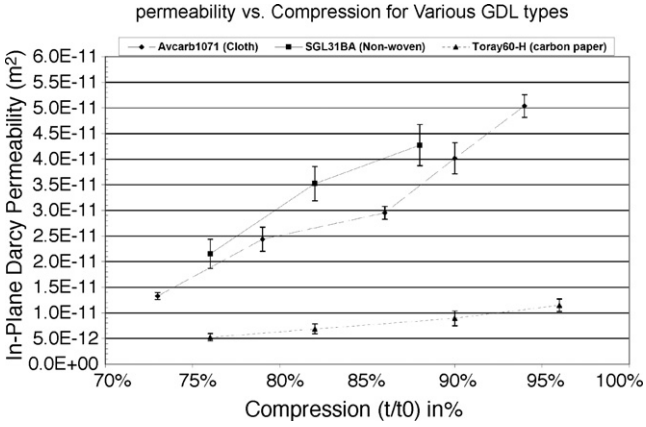

Fig. 6. In-plane permeability of several GDLs.

The correlation between porosity and through plane permeability has been reported by Williams et al. [18]. For various reasons, including its utility in computational studies, it may prove useful to know the relationship between the porosity and in-plane permeability of GDL materials as well. One way to model the relationship between porosity and permeability is through the Kozeny–Carman equation:

$$k_i = C\frac{\phi^3}{(1-\phi)^2} \tag{11}$$

where C is a constant. Strictly, this equation is suited for low porosity materials where the pores have little interaction with one another. In contrast, gas diffusion layers have high porosities (typically >60%) and their pores are highly connected. It has been shown that the Kozeny–Carman equation does not always predict the correct behavior of permeability in fibrous media [17], nevertheless it is generally accurate for small changes in porosity. Therefore, it is interesting to plot permeability against porosity (Fig. 7). The porosity of each experimental data point was estimated from knowledge of the thickness fraction, h/h_0, and the initial porosity, ϕ_0, by the equation:

$$\phi = 1 - \frac{h_0}{h}(1-\phi_0) \tag{12}$$

The value of the initial porosity was obtained from manufacturer's specifications. Porosity specifications for Avcarb 1071-HCB were not available, so it is omitted. Results show that TGP-60-H carbon fiber paper follows the Kozeny–Carman

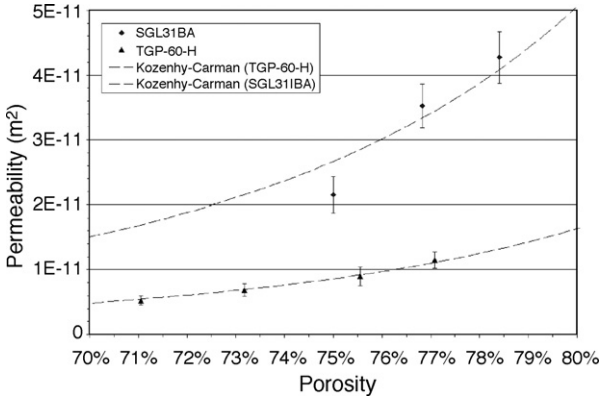

Fig. 7. Experimentally obtained permeability fitted to the Kozeny–Carman equation (Eq. (11)). The computed constants are $C_{\text{TGP-60-H}} = 1.276 \times 10^{-11}$ m^2 and $C_{\text{SGL31BA}} = 3.952 \times 10^{-11}$ m^2.

relationship quite closely. However, SGL31BA does not admit a least-squares fit that falls within the estimated error bounds of the measurement. This is surprising considering that the non-woven material SGL31BA has a similar pore structure to that of the TGP-60-H carbon fiber paper.

5. Conclusions

It has been shown that simple, yet robust radial permeability experiments can be utilized to characterize and differentiate in-plane permeability of gas diffusion layers. These experiments can use either a wetting liquid or a gas of known viscosity as the impregnating fluid and reach identical conclusions. However, the flowrate's dependence on pressure is different for gases and liquids and must be recognized when large pressure differences are present. The model developed here reveals that the flowrate has a quadratic dependence on pressure when compressibility effects are significant whereas the dependence becomes linear for incompressible flow. Results for three commonly used gas diffusion layer materials show that the non-woven material SGL31BA and the carbon fiber cloth material Avcarb 1071-HCB have in-plane permeabilities substantially higher than those reported for other materials throughout the literature.

Acknowledgements

This work was sponsored by W.L. Gore & Associates, and U.S. Department of Energy grant number DEFG0204ER63820. We are grateful to Drs. Will Johnson, Wen Liu, and Uwe Beuscher of W.L. Gore & Associates for their helpful comments and suggestions.

References

[1] M. Williams, R. Kuntz, J. Fenton, Influence of convection through gas diffusion layers on limiting current in PEMFCs using a serpentine flow field, J. Electrochem. Soc. 10 (2004) 1617–1627.

[2] M. Mathias, J. Roth, J. Fleming, W. Lehner, in: W. Vielstich, A. Lamm, H.A. Gasteiger (Eds.), Handbook of Fuel Cells—Fundamentals, Technology and Application, vol. 3, Wiley, 2003 (Chapter 46).

[3] J.P. Feser, A.K. Prasad, S.G. Advani, On the relative influence of convection in serpentine flow fields of PEM fuel cells, J. of Power Sources (2006).

[4] J. Pharaoh, On the permeability of gas diffusion media used in PEM fuel cells, J. Power Sources 144 (2005) 77–82.

[5] T.V. Nguyen, A gas distributor design for proton-exchange-membrane fuel cells, J. Electrochem. Soc. 143 (1996) 105.

[6] W. He, J. Yi, T.V. Nguyen, Two-phase flow model of the cathode of PEM fuel cells using interdigitated flow fields, AIChE 46 (10) (2000) 2053–2064.

[7] G. Hu, J. Fan, S. Chen, Y. Liu, K. Cen, Three-dimensional numerical analysis of proton exchange membrane fuel cells (PEMFCs) with conventional and interdigitated flow fields, J. Power Sources 136 (2004) 1–9.

[8] W. Sun, B. Peppley, K. Karan, Modeling the influence of GDL and flowfield plate parameters on the reaction distribution in the PEMFC cathode catalyst layer, J. Power Sources 144 (2005) 42–53.

[9] K.W. Lum, J.J. McGuirk, 2D and 3D modeling of a PEMFC cathode with interdigitated gas distributors, J. Electrochem. Soc. 152 (4) (2005) A811–A817.

[10] P.M. Wilde, M. Mandle, M. Murata, N. Berg, Structural and physical properties of GDL and GDL/BPP combinations and their influence on PEMFC performance, Fuel Cells 3 (2004) 180–184.

[11] W.K. Lee, C.H. Ho, J.W. Zee, M. Murthy, The effects of compression and gas diffusion layers on the performance of a PEM fuel cell, J. Power Sources 84 (1999) 45–51.

[12] A. Jena, K. Gupta, An innovative technique for pore structure analysis of fuel cell and battery components using flow porometry, J. Power Sources 96 (2001) 214–219.

[13] M. Bluemle, V. Gurau, J. Mann, T. Zawodzinski, E. De Castro, Y.M. Tsou. Permeability and wettability measurements for gas diffusion layers of PEMFCs. In Fuel Cell Seminar: Abstracts, 2004, Poster 53.

[14] K. Adams, L. Rebenfeld, Permeability characteristics of multilayer fiber reinforcements. 1. Experimental observations, Polym. Composites 12 (3) (1991) 179–185.

[15] R.S. Parnas, J.G. Howard, T.L. Luce, S.G. Advani, Permeability characterization. 1. A proposed standard reference fabric for permeability, Polym. Composites 16 (6) (1995) 429–445.

[16] C. Lekakou, M.A.K. Johari, D. Norman, M.G. Bader, Measurement techniques and effects on in-plane permeability of woven cloths in resin transfer moulding, Composites Part A: Appl. Sci. Manuf. 27 (5) (1996) 401–408.

[17] B.T. Astrom, R.B. Pipes, S.G. Advani, On flow through aligned fiber beds and its application to composites processing, J. Composite Mater. 26 (9) (1992) 1351–1373.

[18] M.V. Williams, E. Begg, L. Bonville, R. Kunz, J.M. Fentona, Characterization of gas diffusion layers for PEMFC, J. Electrochem. Soc. 151 (2004) A1173–A1180.